NASA TECHNICAL NOTE

NASA TN D-2335

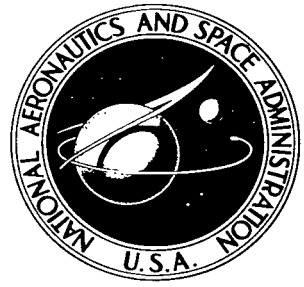

EFFECT OF STAGE SPACING ON PERFORMANCE OF 3.75-INCH-MEAN-DIAMETER TWO-STAGE TURBINE HAVING PARTIAL ADMISSION IN THE FIRST STAGE

by William J. Nusbaum and Robert Y. Wong

Lewis Research Center
Cleveland, Ohio

NATIONAL AERONAUTICS AND SPACE ADMINISTRATION • WASHINGTON, D. C. • JUNE 1964

EFFECT OF STAGE SPACING ON PERFORMANCE OF 3.75-INCH-MEAN-DIAMETER TWO-STAGE TURBINE HAVING PARTIAL ADMISSION IN THE FIRST STAGE

By William J. Nusbaum and Robert Y. Wong

Lewis Research Center
Cleveland, Ohio

NATIONAL AERONAUTICS AND SPACE ADMINISTRATION

For sale by the Office of Technical Services, Department of Commerce,
Washington, D.C. 20230 -- Price $0.75

EFFECT OF STAGE SPACING ON PERFORMANCE OF 3.75-INCH-MEAN-DIAMETER TWO-STAGE TURBINE HAVING PARTIAL ADMISSION IN THE FIRST STAGE

by William J. Nusbaum and Robert Y. Wong

Lewis Research Center

SUMMARY

The design and the experimental investigation of a 3.75-inch-mean-diameter partial-admission two-stage turbine are presented herein. The investigation was made to determine the effect on two-stage-turbine performance of a change in the axial distance between stages for a turbine with partial admission in the first stage. Accordingly, the turbine was designed with 31.3-percent admission in the first stage, full admission in the second stage, and provision for changing the axial distance between stages. The results of the two-stage investigation are presented for each of the axial distances between stages of 0.25, 0.50, 0.75, 1.00, 1.50, and 2.00 inches. The results of the first-stage investigation are also presented, together with a calculated efficiency for the second stage, at each value of stage spacing as calculated from the two-stage and first-stage results.

The results of the two-stage investigation showed that the performance of the turbine was penalized severely by the comparatively small arc of admission in the first stage when the distance between stages was small. There was, however, an increase of 7.1 points in efficiency as the distance between the stages was increased from 0.25 to 2.00 inches, efficiency reaching the design value of 0.655 at the latter distance and at the design blade- to jet-speed ratio. This increase in efficiency was due to an improved circumferential distribution of flow into the second stage at the greater distance, as evidenced by the interstage pressure measurements. As a result of the better flow distribution, the efficiency of the second stage increased 7.2 points when the stage spacing was increased from 0.25 to 2.00 inches.

INTRODUCTION

A large number of propulsion systems make use of small, turbine-driven power units with outputs of 1 to 100 horsepower. The working fluid for these turbines may be at pressures of several hundred pounds per square inch. The

combination of low power output and high inlet pressures necessitates a turbine design with extremely low volume flow at the turbine inlet. This requirement of low volume flow usually leads to a design compromise between blade height and arc of admission. The blade height of a full-admission design may be too short to be practical, while partial admission will result in circumferential pressure gradients. These circumferential gradients present no particular problem for single-stage turbines. For multistage turbines, however, these gradients may affect appreciably the downstream full-admission stages when sufficient spacing is not provided for proper distribution of the flow.

In order to study this effect with a comparatively large pressure gradient, a turbine was designed and was evaluated at the Lewis Research Center. This turbine was designed as a two-stage axial-flow unit with a constant mean diameter of 3.75 inches, 31.3-percent admission in the first stage, and full admission in the second stage.

This report presents the design and the results of a cold-air performance investigation of the subject turbine over a range of blade- to jet-speed ratios from 0.10 to 0.29 for each of the axial distances between stages of 0.25, 0.50, 0.75, 1.00, 1.50, and 2.00 inches. This report also presents the results of a cold-air performance investigation of the first stage only and the efficiency of the second stage as calculated from the single- and two-stage results.

SYMBOLS

D_p pressure-surface diffusion parameter, [(blade-inlet relative velocity) - (minimum blade-surface relative velocity)]/blade-inlet relative velocity

D_s suction-surface diffusion parameter, [(maximum blade-surface relative velocity) - (blade-outlet relative velocity)]/maximum blade-surface relative velocity

D_{tot} sum of suction- and pressure-surface diffusion parameters, $D_p + D_s$

g gravitational constant, 32.17 ft/sec^2

Δh specific work output, Btu/lb

hp horsepower

J mechanical equivalent of heat, 778 ft-lb/Btu

K(A/W) loss coefficient of ref. 1, equivalent to C of ref. 2

p absolute pressure, lb/sq ft

r_{le} leading-edge radius, in.

r_{te} trailing-edge radius, in.

U blade velocity, ft/sec

V absolute gas velocity, ft/sec

W relative gas velocity, ft/sec

w weight-flow rate, lb/sec

γ ratio of specific heats

δ ratio of turbine-inlet total pressure to that of U.S. standard sea-level atmosphere, $p_0'/2116.22$

ϵ function of γ used in relating weight flow to that using inlet conditions at U.S. standard sea-level atmosphere, $\frac{0.740}{\gamma}\left(\frac{\gamma+1}{2}\right)^{\gamma/(\gamma-1)}$

η adiabatic efficiency, ratio of blade power to ideal blade power based on inlet total- to exit static-pressure ratio

θ_{cr} squared ratio of critical velocity at turbine inlet to critical velocity at U.S. standard sea-level atmosphere, $(V_{cr,0}/1019.46)^2$

λ speed-work parameter, $U_m/gJ\,\Delta h$

ν blade- to jet-speed ratio, $U_m/\sqrt{2gJ\,\Delta h_{id}}$

φ blade stagger angle, see table I

Subscripts:

cr conditions at Mach number of unity

id ideal

m mean radius

x axial direction

0 station at turbine inlet collector (figs. 2 and 7)

1 station at turbine inlet (fig. 2)

2 station just upstream of trailing edge of first-stage stator

3 station between first-stage stator and rotor

4 station just downstream of leading edge of first-stage rotor

5 station just upstream of trailing edge of first-stage rotor

6 station between first-stage rotor and second-stage stator

7 station just upstream of leading edge of second-stage stator

8 station just upstream of trailing edge of second-stage stator

9 station between second-stage stator and rotor

10 station just downstream of leading edge of second-stage rotor

11 station just upstream of trailing edge of second-stage rotor

12 station downstream of second-stage rotor

Superscript:

' absolute total state

TURBINE DESIGN

Design Requirements

The design requirements for the 3.75-inch-mean-diameter two-stage partial-admission turbine were as follows:

Overall equivalent specific work output, $\Delta h/\theta_{cr}$, Btu/lb	43.6
Overall blade- to jet-speed ratio, ν	0.27
Equivalent weight flow, $\epsilon w\sqrt{\theta_{cr}}/\delta$, lb/sec	0.060
Overall speed-work parameter, λ	0.221
Equivalent horsepower, $\epsilon hp/\delta\sqrt{\theta_{cr}}$	3.7
Equivalent mean-blade-section velocity, $U_m/\sqrt{\theta_{cr}}$, ft/sec	490.9
First-stage admission, percent	31.3
Second-stage admission, percent	100

Velocity Diagrams

The free-stream velocity diagrams were computed to meet the design requirements and are based on the following assumptions:

(1) Equal values of speed-work parameter per stage of 0.44

(2) A one-third and two-third split of total-pressure loss between the stator and rotor, respectively, for each stage

(3) A total-pressure loss between stages equal to the kinetic energy leaving the first stage

(4) Uniform flow into the second stage

Design total-to-total efficiency for each stage was obtained from an experimen-

tally obtained loss coefficient and equation (8) of reference 1. The loss coefficient K(A/W) of equation (8) (ref. 1), which is equivalent to C of reference 2, was obtained from experimental data presented in reference 2. The basic loss coefficient K(A/W) or C used was 0.216. The resulting total-to-total efficiencies of 0.690 and 0.635 were used for the first and second stages, respectively; they resulted in an overall total-to-total efficiency of 0.679. The corresponding design total-to-static efficiencies used were 0.645 and 0.588 for the first and second stages, respectively, and the overall static efficiency was 0.655. The resulting design overall total-to-total pressure ratio and the overall total- to static-pressure ratio were 12.6 and 14.5, respectively.

The free-stream velocity diagrams and a sketch of the blading showing the station nomenclature are shown in figures 1 and 2, respectively. There is com-

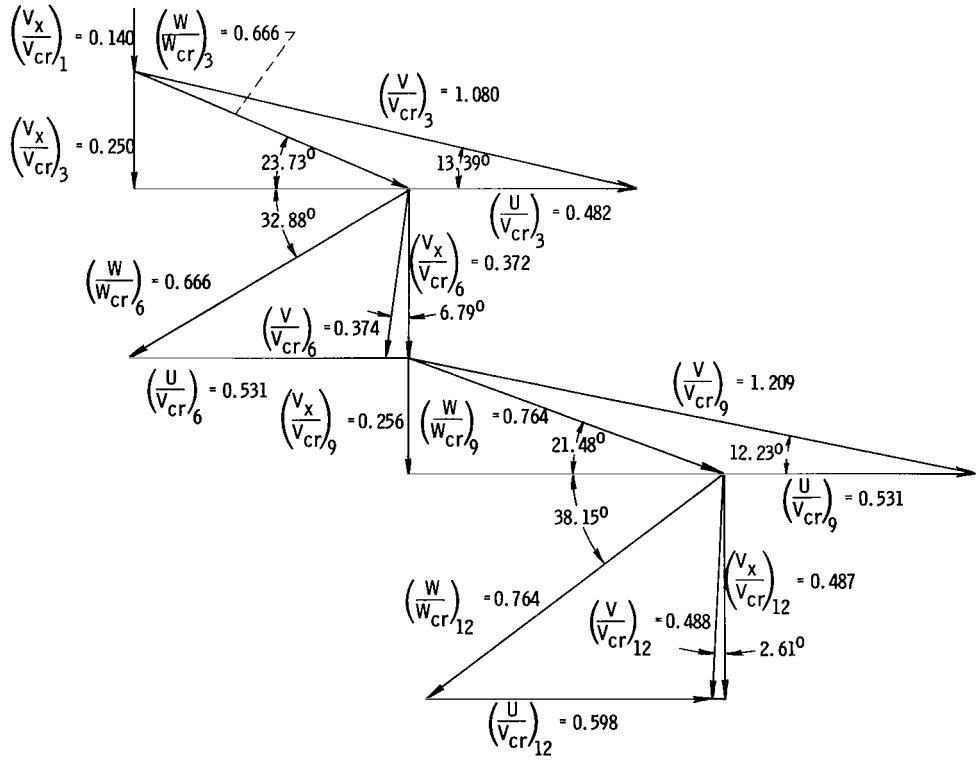

Figure 1. - Free-stream velocity diagrams.

paratively large turning in both stators with exit angles measured from the tangential direction of 13.39° and 12.23° for the first and second stages, respectively. The stator exit velocities are slightly supersonic, the critical velocity ratios V/V_{cr} being 1.080 and 1.209, respectively. Both rotors were designed for equal inlet and outlet relative critical velocity ratios W/W_{cr} of 0.666 and 0.764 for the first and second stages, respectively. The design turning in the first rotor is 123.39°, and that in the second rotor is 120.37°; there is a small amount of negative exit whirl out of each stage.

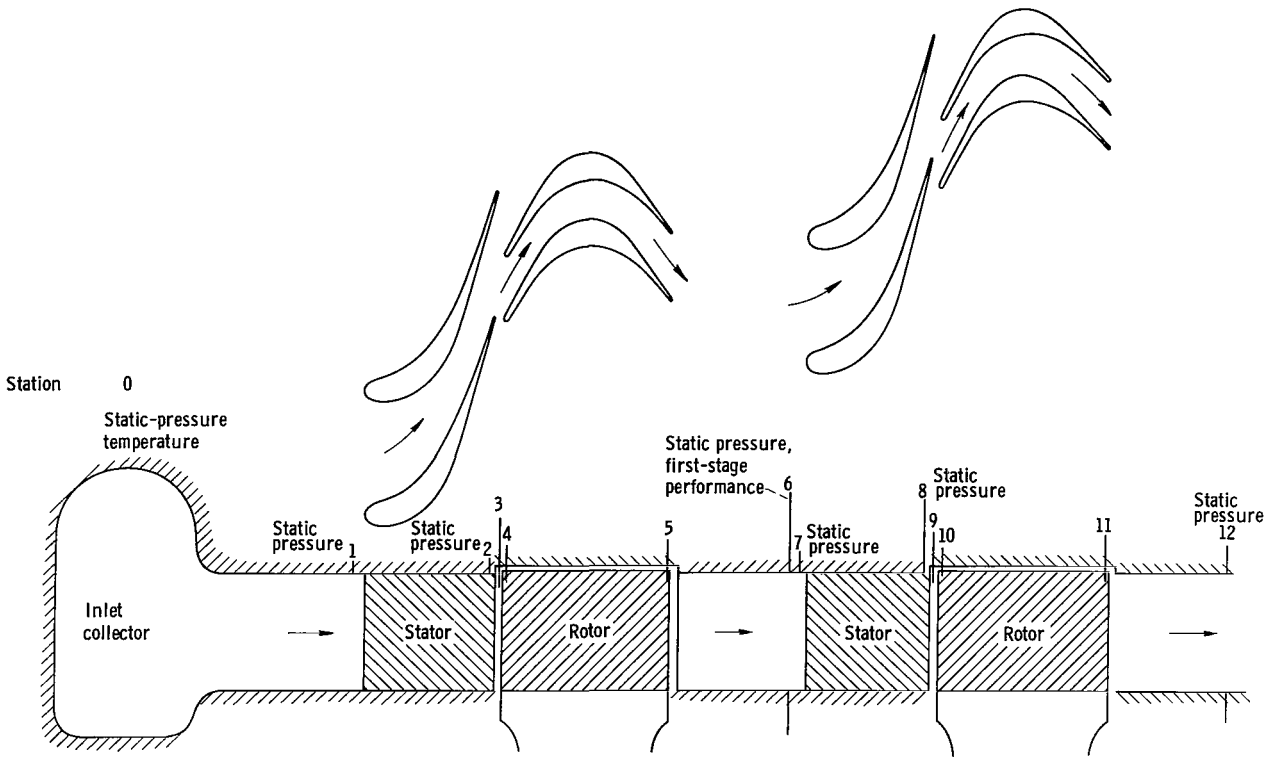

Figure 2. - Stator- and rotor-blade profiles and flow passage with station nomenclature.

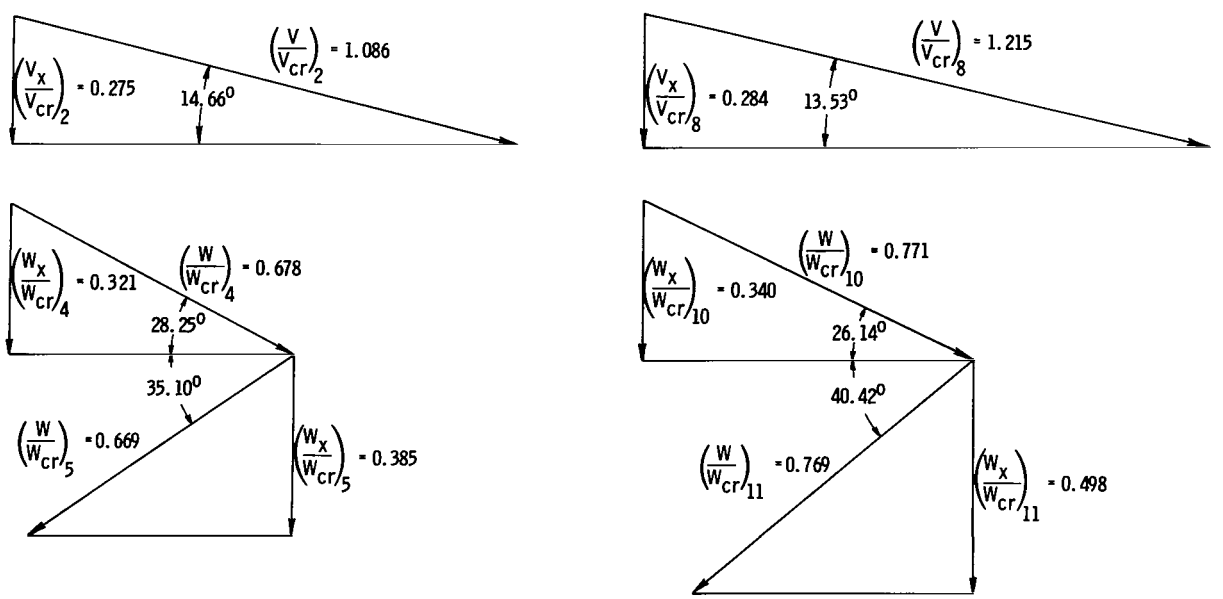

Figure 3. - Blade-design velocity diagrams. (See fig. 2 for station nomenclature.)

Velocity diagrams for use in the blade design were computed for stations 2, 4, 5, 8, 10, and 11 from the free-stream velocity diagrams at stations 3, 6, 9, and 12 and are based on the following assumed conditions between adjacent stations:

(1) No change in the tangential component of velocity

(2) No loss in total pressure

(3) Continuity

The blade-design velocity diagrams are shown in figure 3. These diagrams were calculated for a first-stage stator consisting of 16 blades in an arc of admission of 112.8° and a second-stage, full-admission stator of 51 blades. Both stators have a blade trailing-edge radius of 0.0024 inch and a constant blade height of 0.217 inch. The calculations for both rotors were based on 95 blades with a leading-edge radius of 0.005 inch and a trailing-edge radius of 0.0025 inch.

Stators

The first-stage stator-blade-section profile was first laid out to give a smoothly converging channel and a straight suction surface downstream of the throat. The analysis method of reference 3 was then used to predict the midchannel and blade-surface gas-velocity distributions. In this analysis the total-pressure loss across the blade row was assumed to occur linearly in the axial direction between the blade inlet and the throat. Both the blade-section profile and the stagger angle were specified constant from hub to tip. Then, by an iterative process, wherein the blade profile upstream of the throat was varied, a blade profile with the desired velocity distribution was obtained. The coordinates of the resulting stator blade are shown in table I. The value of the stagger angle for this first-stage stator was 57°27'. The blade profile as designed for the first-stage stator was also used for the second-stage stator but at the slightly different stagger angle of 59°9'. The midchannel and blade-surface gas-velocity distributions were then predicted for the second-stage stator. The resulting velocity distributions for the two stators gave approximately the same values of diffusion, these values being 0 and 0.2 for the suction- and pressure-surfaces, respectively. The stator-blade profile and the first- and second-stage stator channels are shown in figure 2. The solidity of both stators is 1.96. This stator blade has a comparatively small trailing-edge radius of 0.0024 inch, which gives blockage values of 8.3 and 9.4 percent for the first and second stages, respectively. Design parameters for the stator blading are summarized in table II.

Rotors

The rotor-blade profiles were first laid out with a straight suction surface both upstream and downstream of the guided channel; the resulting flow passage had a gradually increasing width from the entrance to the region of

TABLE I. - STATOR-BLADE COORDINATES

[First-stage stator-blade stagger angle, 57°27'; second-stage stator-blade stagger angle, 59°9'.]

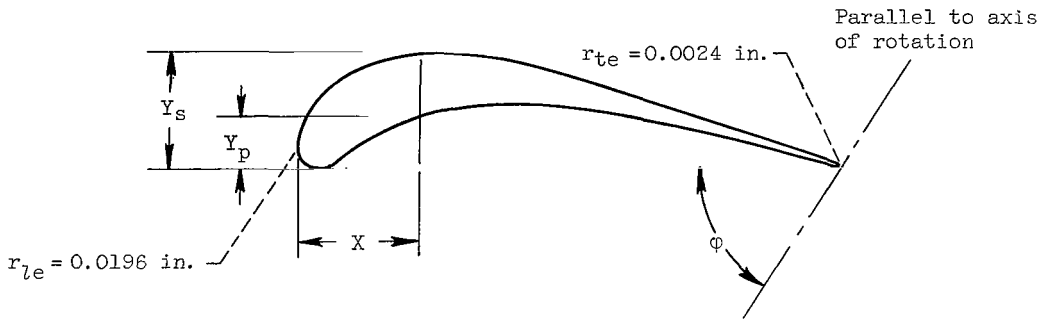

X, in.	Y_p, in.	Y_s, in.	X, in.	Y_p, in.	Y_s, in.
0	0.0196	0.0196	0.240	0.052	0.074
.030	.003	.066	.270	.047	.064
.060	.026	.085	.300	.041	.054
.090	.041	.094	.330	.034	.044
.120	.050	.097	.360	.027	.034
.150	.055	.095	.390	.018	.025
.180	.057	.091	.420	.010	.015
.210	.056	.083	.453	.0024	.0024

TABLE II. - DESIGN PARAMETERS

Turbine stage	Blade row	Blade-surface diffusion parameter			Admission, percent	Number of blades	Solidity	Aspect ratio	Trailing-edge blockage, percent
		Suction surface, D_s	Pressure surface, D_p	Total, D_{tot}					
First	Stator	0	0.2	0.2	31.3	16	1.96	0.48	8.3
	Rotor	0.098	0.521	0.619	----	95	2.5	0.70	7.0
Second	Stator	0	0.2	0.2	100	51	1.96	0.48	9.4
	Rotor	0.087	0.565	0.652	---	95	2.6	0.68	6.2

maximum curvature and then a slightly decreasing width to the channel exit. The analysis method of reference 3 was used to predict blade surface velocities. In this analysis the total-pressure drop across the blade row was assumed to occur linearly in the axial direction between the blade inlet and the exit of the guided channel. Both the blade-section profile and the stagger angle were specified constant from hub to tip. Then, by an iterative process wherein the solidity and blade shape forming the guided channel were varied, the profile with the desired velocity distribution and diffusion parameter was obtained. The rotor-blade profiles and the first- and second-stage rotor chan-

nels are shown in figure 2. As shown in the figure, the blades of both rotors extended into a recess in the turbine casing. This recess allowed for an extension of about 0.007 inch with a tip clearance of about 0.005 inch. As reported in reference 4, this type of configuration at the rotor-blade tips is effective in reducing tip clearance losses. The coordinates for the first- and second-stage rotor blades are given in table III. An unusual design feature of

TABLE III. - ROTOR-BLADE COORDINATES

[First-stage stagger angle, 7°5'; second-stage stagger angle, 13°25'.]

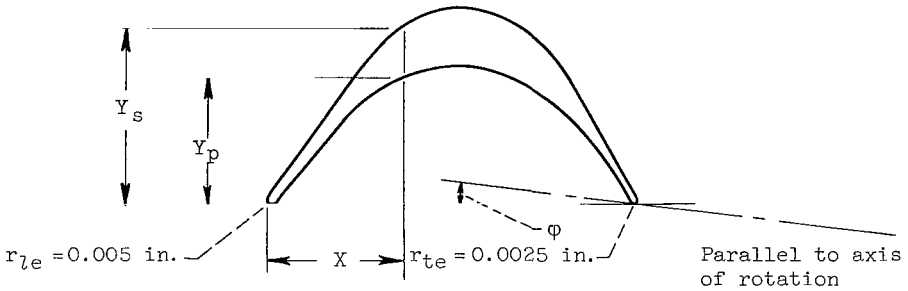

First stage			Second stage		
X, in.	Y_p, in.	Y_s, in.	X, in.	Y_p, in.	Y_s, in.
0	0.005	0.005	0	0.005	0.005
.020	.017	.035	.020	.015	.031
.040	.045	.063	.040	.039	.055
.060	.069	.091	.060	.064	.079
.080	.088	.118	.080	.084	.103
.100	.103	.141	.100	.100	.125
.120	.113	.157	.120	.111	.143
.140	.119	.167	.140	.118	.158
.160	.121	.172	.160	.122	.167
.180	.120	.171	.180	.123	.170
.200	.115	.165	.200	.119	.168
.220	.106	.152	.220	.112	.160
.240	.093	.132	.240	.099	.143
.260	.075	.101	.260	.082	.116
.280	.049	.063	.280	.058	.078
.300	.015	.026	.300	.026	.038
.312	.0025	.0025	.3177	.0025	.0025

these blades is the thin trailing edges (radius, 0.0025 in.), which gave blockage values of 7.0 and 6.2 percent for the first- and second-stages, respectively. The calculated blade-surface and midchannel velocity distributions are shown in figures 4(a) and (b) for the first- and second-stage rotors, respectively. The comparatively low values of the suction-surface diffusion parameter D_s are 0.098 and 0.087 for the first and second stages, respectively. The pressure surface of the first-stage rotor has a diffusion parameter D_p of 0.521, and thus the total diffusion parameter D_{tot} is 0.619. The second-stage rotor has a pressure surface diffusion of 0.565 and a total diffusion of

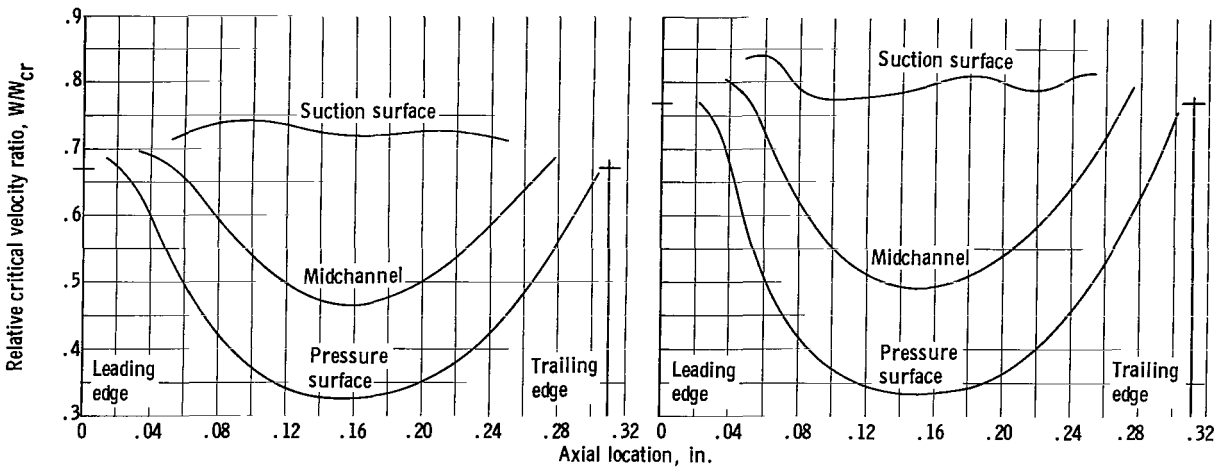

(a) First-stage rotor. (b) Second-stage rotor.

Figure 4. - Design rotor midchannel and surface velocity distributions as function of axial location.

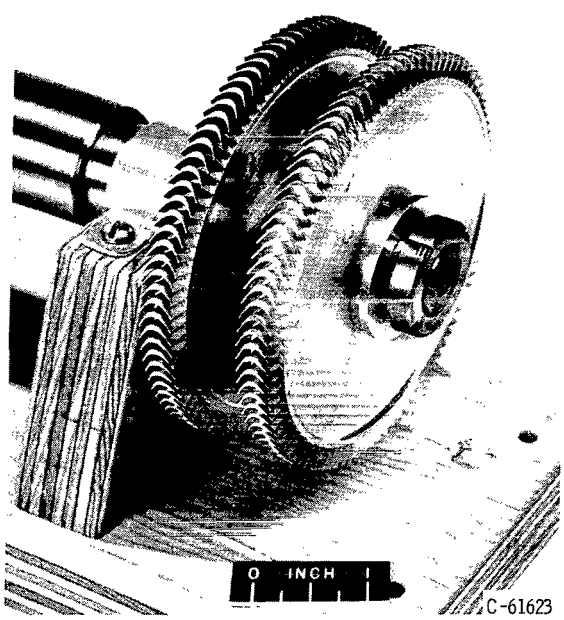

Figure 5. - Turbine rotors.

0.652. The design solidities are 2.5 and 2.6 for the first- and second-stage rotors, respectively. An overall view of the two rotor assemblies is shown in figure 5. Design parameters for the rotor blading are summarized in table II.

APPARATUS, INSTRUMENTATION, AND PROCEDURE

The apparatus used in this investigation consisted of the turbine described in the preceding section, an airbrake to absorb and measure the output of the turbine, and two separate systems of piping and controls to provide the desired inlet conditions to both the turbine and the airbrake and exhaust conditions from the turbine. Figure 6 shows an overall view of the experimental turbine installation. High-pressure dry air was supplied from the laboratory air system, was heated to 610° R by an electric heater, was filtered to remove dirt particles, and then was piped into the turbine. After passing through the turbine, the air was exhausted through the pipe shown in figure 6 and into the laboratory low-pressure exhaust system. By means of remotely controlled and regulated valves, the inlet pressure was maintained at a constant value while the exhaust pressure was varied in order to obtain the desired pressure ratios across the turbine. Flow to the airbrake was supplied from the laboratory air system, which was maintained at approximately 40 pounds per square inch gage. After the air was throttled to the desired pressure, it

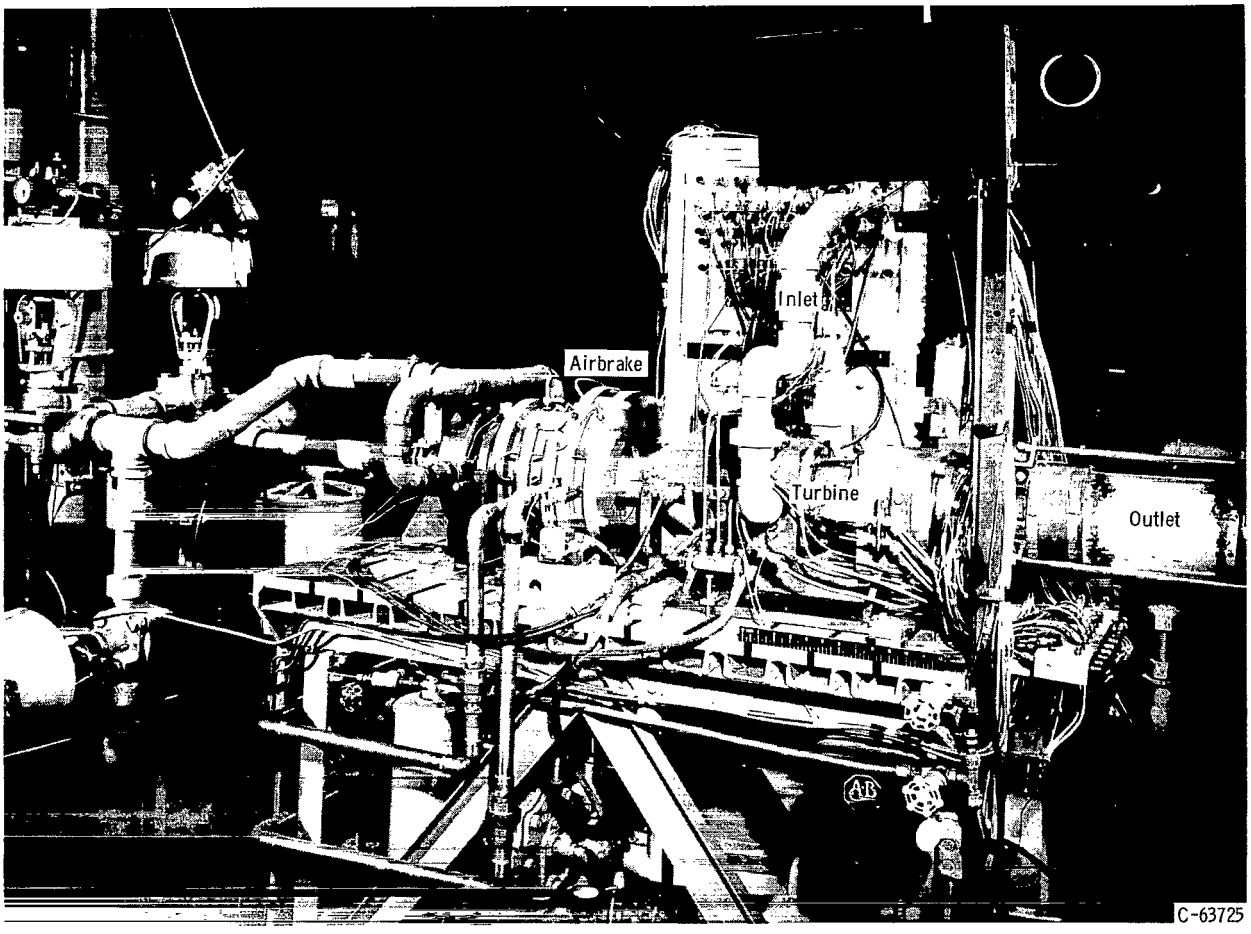

Figure 6. - Turbine test apparatus.

passed through the system of piping into the inlet manifold, through the airbrake, and then discharged axially into the test cell. A cutaway view of the airbrake is presented in reference 5; a description of a similar airbrake is presented in reference 6.

A cutaway drawing of the turbine assembly is shown in figure 7. The air enters the turbine through the inlet collector, passes through the open section of the first-stage stator, the first-stage rotor, an annular passage of constant flow area, the second-stage blading, and the outlet pipe. The drawing shows the two stages at their closest position (0.25 in.). By inserting spacers in both the inner and the outer walls and the rotor shaft, however, the second stage could be moved axially, in steps, to a distance of 2.00 inches. As the second stage was moved, all second-stage static-pressure taps remained in the same position relative to that stage.

Instrumentation was provided to obtain overall performance and static pressures between blade rows. The airflow was measured by a calibrated orifice plate. The torque output of the turbine was measured with a calibrated strain-gage-type load cell. The rotational speed of the turbine was measured with an

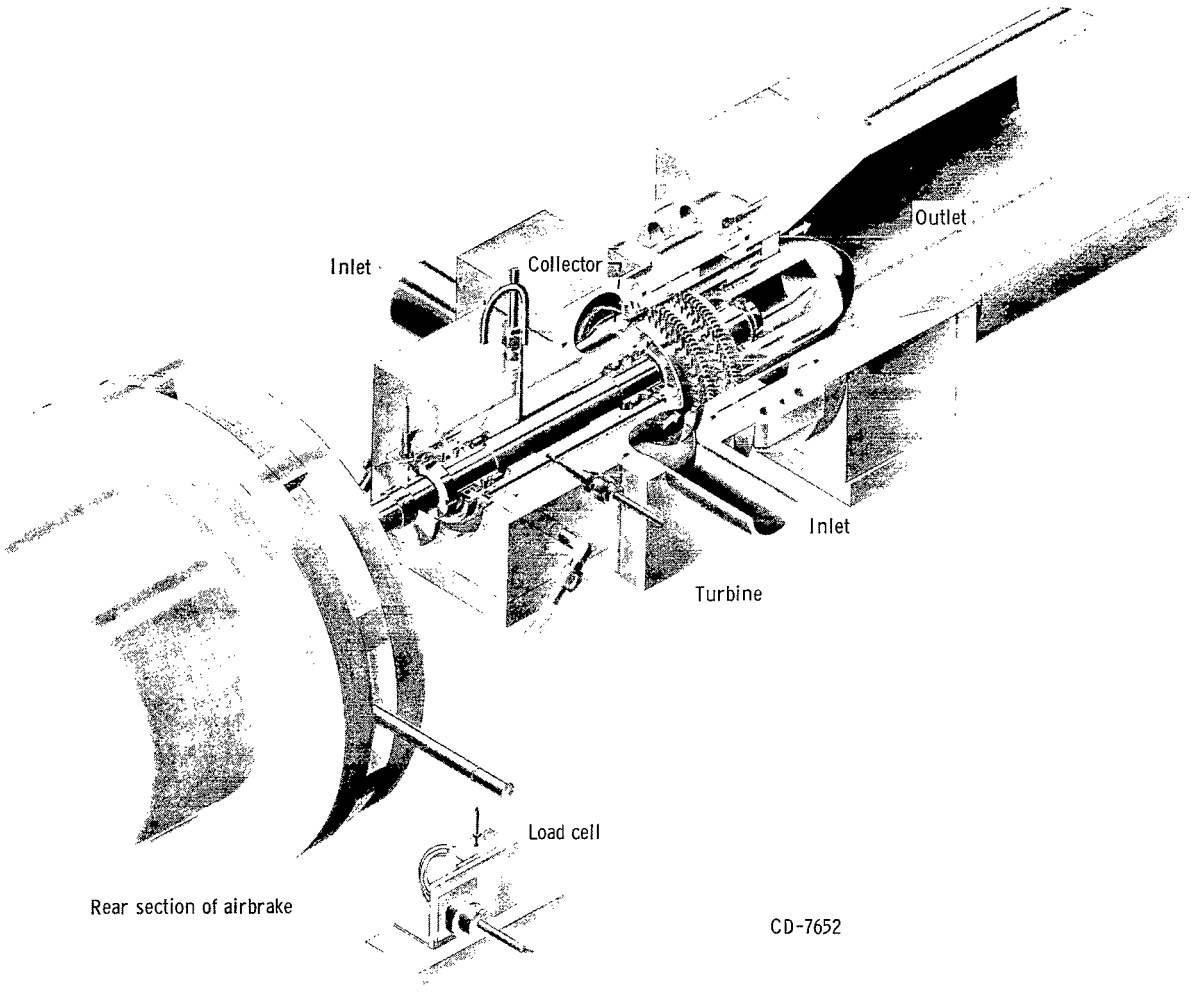

Figure 7. - Cutaway view of turbine assembly with section of airbrake.

electronic counter in conjunction with a magnetic pickup and a shaft-mounted gear. Static-pressure measurements at each of the stations 1, 2, 7, and 8 (fig. 2) were made by calibrated electrical pressure transducers from four taps spaced approximately 90° apart around the outer wall and midway between adjacent blades. The turbine-inlet total pressure was measured with two static-pressure taps, which were located in the inlet collector (station 0) 180° apart at points of low Mach number where the total- to static-pressure ratio was assumed equal to 1.0. Turbine overall performance was based on an average of the static pressures measured by mercury manometer tubes from 12 static-pressure taps located immediately downstream of the second-stage rotor trailing edge (station 12). These taps were equally spaced around the annulus, six on the inner wall and six on the outer wall. The first-stage performance was based on an average of the pressures at station 6 as measured by calibrated electrical pressure transducers from 12 static-pressure taps located immediately downstream of the rotor-blade trailing edge. These taps were equally spaced around the annulus, six on the inner wall and six on the outer wall. Temperatures were measured with two thermocouples 180° apart in the inlet collector. All

data recorded by an automatic digital potentiometer were processed through an electronic computer.

Experimental data for the two-stage operation were taken for each of the configurations, in which the axial distance between the first and second stage was 0.25, 0.50, 0.75, 1.00, 1.50, and 2.00 inches. Data were taken over a range of inlet-total- to exit-static-pressure ratios from 8 to 17.

For the single-stage test, data were taken for values of pressure ratio across the stage of 2.5, 3.0, and 3.5. At each pressure ratio, the turbine rotor speed was varied from about 13,000 to 33,500 rpm. The average turbine-inlet temperature was about 600° R, and the inlet total pressure was approximately 60 pounds per square inch absolute.

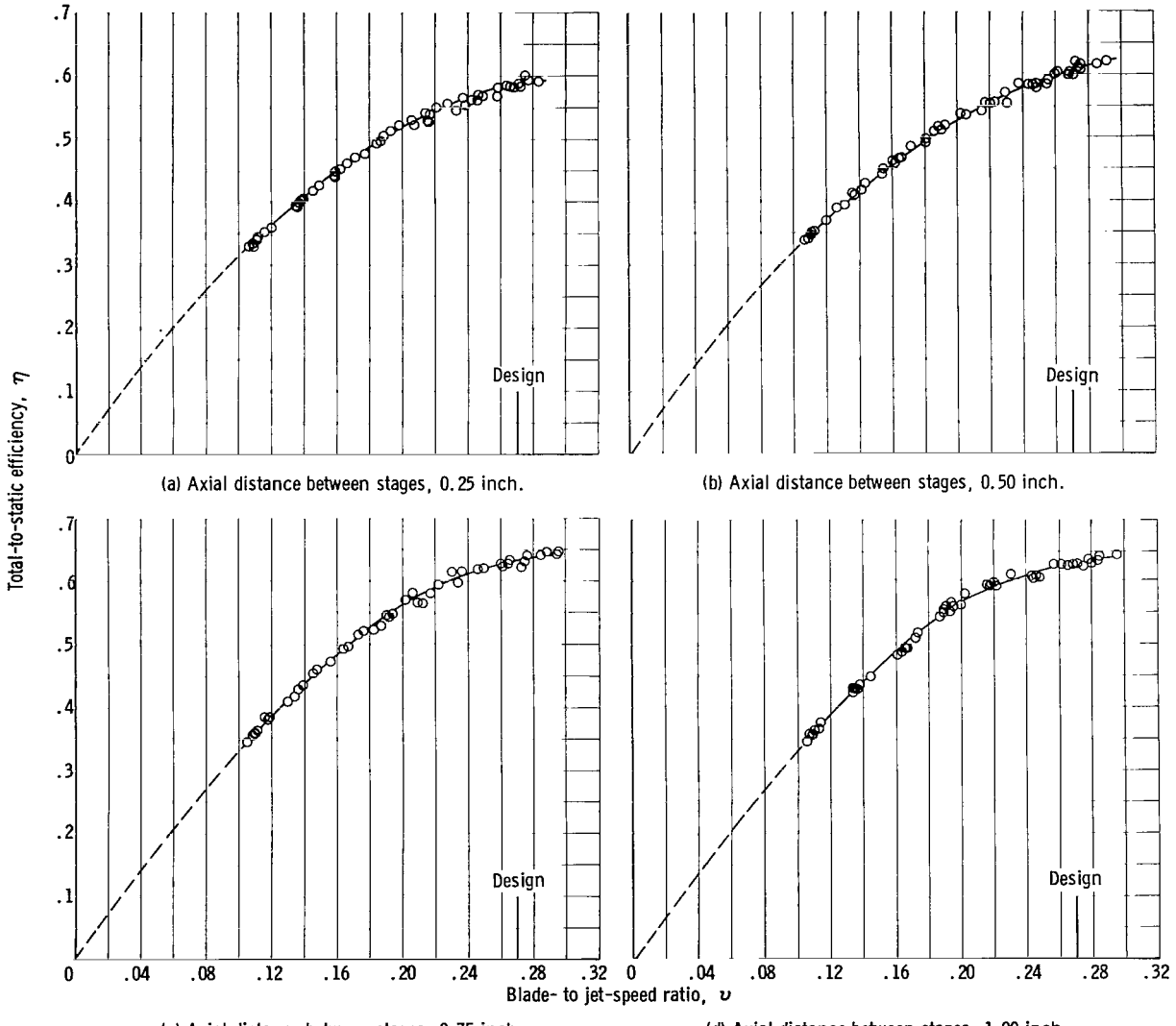

Figure 8. - Performance characteristics of two-stage turbine.

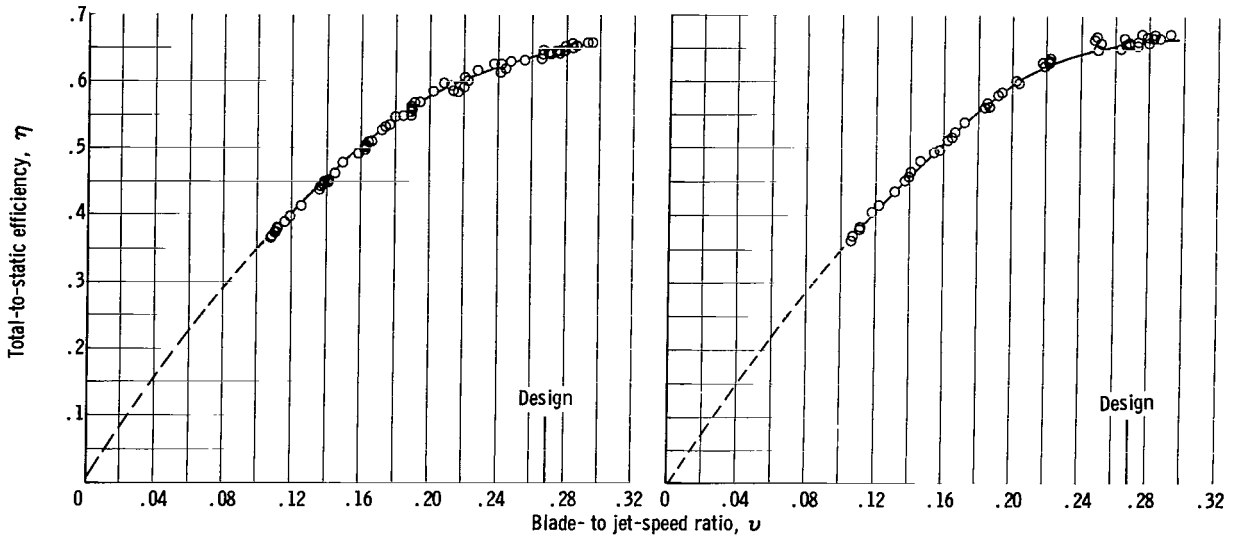

(e) Axial distance between stages, 1.50 inches.

(f) Axial distance between stages, 2.00 inches.

Figure 8. - Concluded. Performance characteristics of two-stage turbine.

The friction torque of the bearings and seals was obtained by motoring the shaft at various speeds and measuring the torque with a strain-gage load cell. Then the friction power calculated from this torque was added to the shaft power to obtain the turbine rotor power. The turbine efficiency was computed as the ratio of actual rotor output to ideal output, the latter having been calculated from the weight flow, the inlet total temperature and pressure, and the outlet static pressure.

RESULTS AND DISCUSSION

Overall Performance

The performance characteristics of the subject two-stage turbine are presented in figure 8. This figure shows the variation of total-to-static efficiency η with blade- to jet-speed ratios from about 0.11 to 0.29 for each of the axial distances between stages of 0.25, 0.50, 0.75, 1.00, 1.50, and 2.00 inches. For the range of axial distances considered, it can be observed that there is a tendency toward increased efficiency with increase in distance between stages at all values of blade- to jet-speed ratio. At the design value of blade- to jet-speed ratio ν of 0.27, values of efficiency were read from figure 8 and plotted as functions of distance between stages in figure 9. There is an increase in efficiency from a value of 0.584 at a distance of 0.25 inch to a value

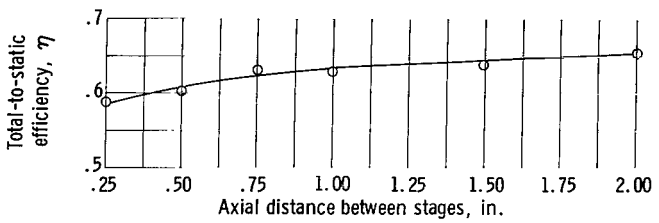

Figure 9. - Two-stage performance at design blade- to jet-speed ratio.

of 0.655 at a distance of 2.00 inches. Operation of the turbine at the latter point resulted in an overall equivalent specific work output $\Delta h/\theta_{cr}$ of 43.6 Btu per pound, which also is the design value. The rate of change of efficiency with distance, as indicated by the slope of the curve, is greatest at a distance near 0.25 inch, decreases as the distance increases, and becomes constant for values of distance greater than 1.00 inch. It is believed, however, that the efficiency should reach a maximum value at some distance and that further increases in distance will result in a decrease in efficiency because of increased wall friction losses.

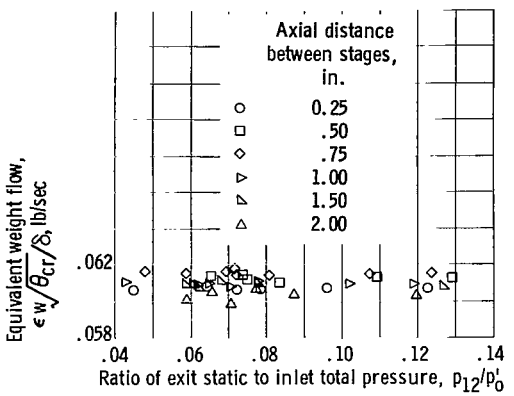

Figure 10. - Variation of equivalent weight flow with ratio of exit static to inlet total pressure at design speed.

Weight-flow characteristics at design speed are presented in figure 10. In this figure equivalent weight flow $\epsilon w(\sqrt{\theta_{cr}}/\delta)$ is plotted as a function of the ratio of exit static to inlet total pressure for each of the six configurations investigated. It can be seen that the equivalent weight flow is essentially constant over the range of pressure ratios for all configurations, which indicates that the turbine is choked. Since a study of the test data for all speeds also shows that the weight flow did not vary with speed, it is concluded that the first-stage stator was choked. The figure shows an average value of equivalent weight flow of 0.061 pound per second, which is about 1.7 percent larger than the design value of 0.060 pound per second. Since the measured value of the first-stage stator throat area was about 1.2 percent smaller than the design value, the results indicate a first-stage flow coefficient of 0.982 instead of the design value of 0.95.

Pressure Distribution

An indication of the circumferential mass flow gradient through the turbine can be obtained from a study of the pressure distribution. Accordingly, figure 11 presents the variation of the ratio of local static pressure to inlet total pressure p/p'_0 with station number for each of four configurations (distance between stages of 0.25, 0.75, 1.50, and 2.00 in.) and for each of the four equally spaced circumferential tap locations a, b, c, and d. (The two configurations having distances between stages of 0.50 and 1.00 in. are not included because of the failure of several pressure transducers.) The design pressure distribution as calculated for the active section of the turbine is also presented. It should be noted that tap location a is in approximately the same circumferential position as the midpoint of the active section of the first-stage stator, whereas the other three tap locations are in circumferential positions corresponding to the blocked section of this stator. For tap location a (fig. 11(a)), it can be observed that the design pressure ratio was not obtained across either stage for any of the configurations. As the distance between stages was increased, however, these pressure ratios did approach

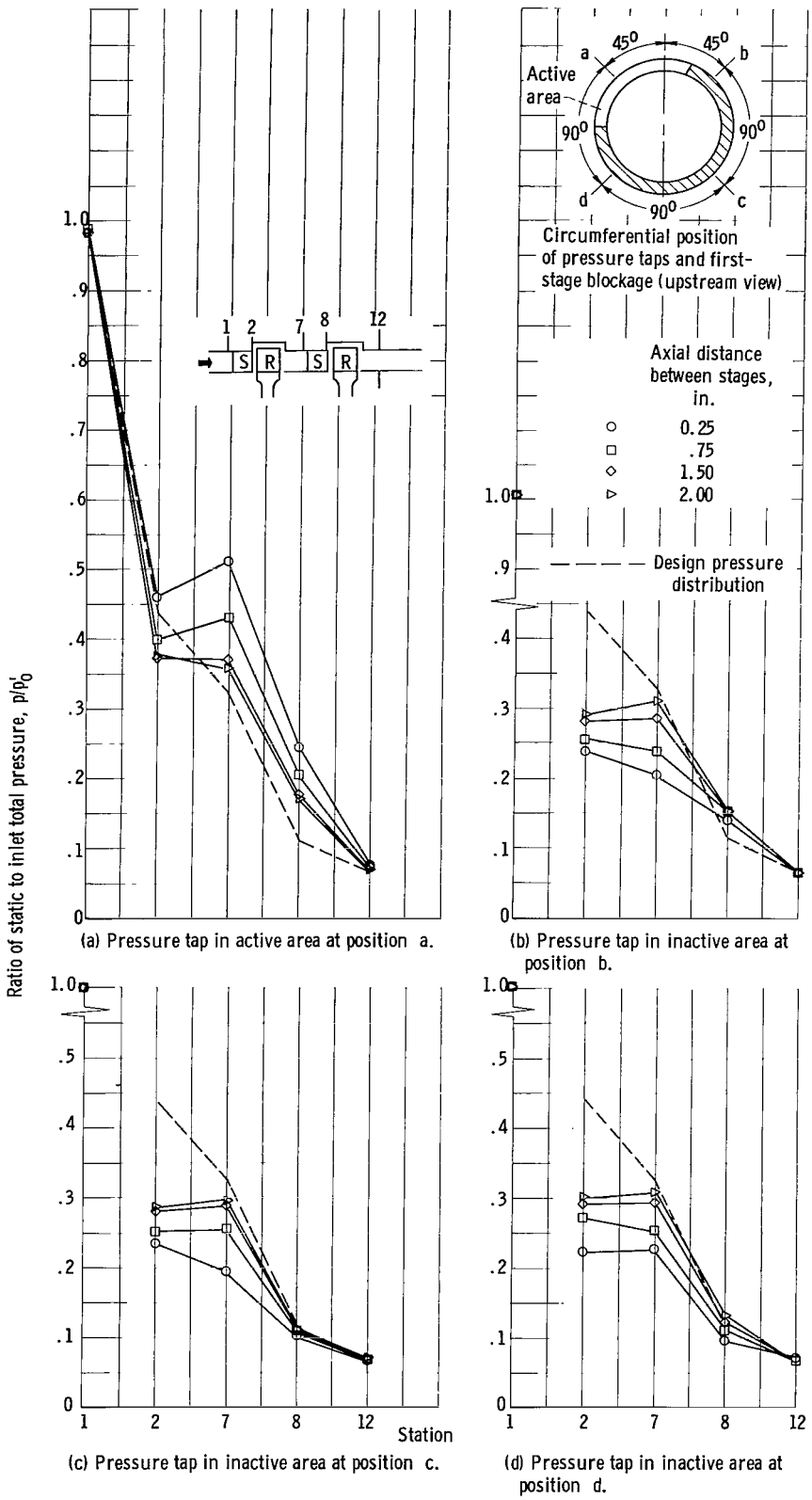

(a) Pressure tap in active area at position a.

(b) Pressure tap in inactive area at position b.

(c) Pressure tap in inactive area at position c.

(d) Pressure tap in inactive area at position d.

Figure 11. - Variation of static pressure through turbine at design speed and overall pressure ratio.

the design values. The interstage static pressure was larger than design because of the failure of the air jet from the active section of the first stage to be properly distributed circumferentially before entering the second stage. Thus, this jet was required to pass through a small segment of the second stage. Since the area in this segment is too small to pass the weight flow at design pressure, continuity requires that this pressure be larger than design. As the axial distance between stages was increased, the air jet from the active section of the first stage became more evenly distributed circumferentially and the flow area was thereby increased and continuity maintained at a pressure level closer to the design value. The pressure ratio across the second stator was about 2.1 as compared with the design value of 2.85 and did not vary appreciably with axial distance between stages. This low value of pressure ratio may be attributed to a choked condition in the second-stage rotor, which resulted from a throat area 3.1 percent less than design. Figure 11(a) also shows that the pressure ratio across the first-stage stator increased with axial distance between stages and reached a maximum value larger than design. This increase in pressure ratio is due to a better circumferential distribution of flow between stages, as discussed previously. Since the pressure ratio had a maximum value that was larger than the design value, it is indicated that the first-stage rotor throat area is too large. At the same time, the reaction across the rotor increased as the distance between stages increased and changed from negative to positive values at a distance of about 1.5 inches but never reached design reaction. The second-stage rotor, however, operated at reaction greater than design, and the reaction decreased with an increase in axial distance between stages. This high reaction was caused by the large concentration of flow behind the active area of the first-stage stator, as discussed previously. As the distance between stages was increased, the flow gradients were decreased, and there resulted a decrease in the reaction across the rotor in the active area.

Pressures measured at b, c, and d behind the inactive region are shown in figures 11(b), (c), and (d), respectively. In these figures the data points at stations 1 and 2 are not connected because there is no flow between these points. At each circumferential tap position the pressures were generally lower than design at all stations and for all axial distances but increased with an increase in axial distance. These low pressures are indicative of the low weight flows in these regions and show further the tendency to approach design values as the distance between stages is increased. The same pressures are presented in figure 12, where the ratio of local static to inlet total pressure is presented as a function of circumferential position for each station and for each axial distance between stages. This figure further illustrates the beneficial effect of increased axial distance on circumferential flow distribution. As the axial distance is increased, the pressures approach a constant value for each of the stations 2, 7, and 8, as shown in figures 12(a), (b), and (c), respectively. At station 12 (fig. 12(d)) there is a fairly uniform flow distribution for all distances.

Stage Performance

The performance characteristics of the first stage of the subject turbine

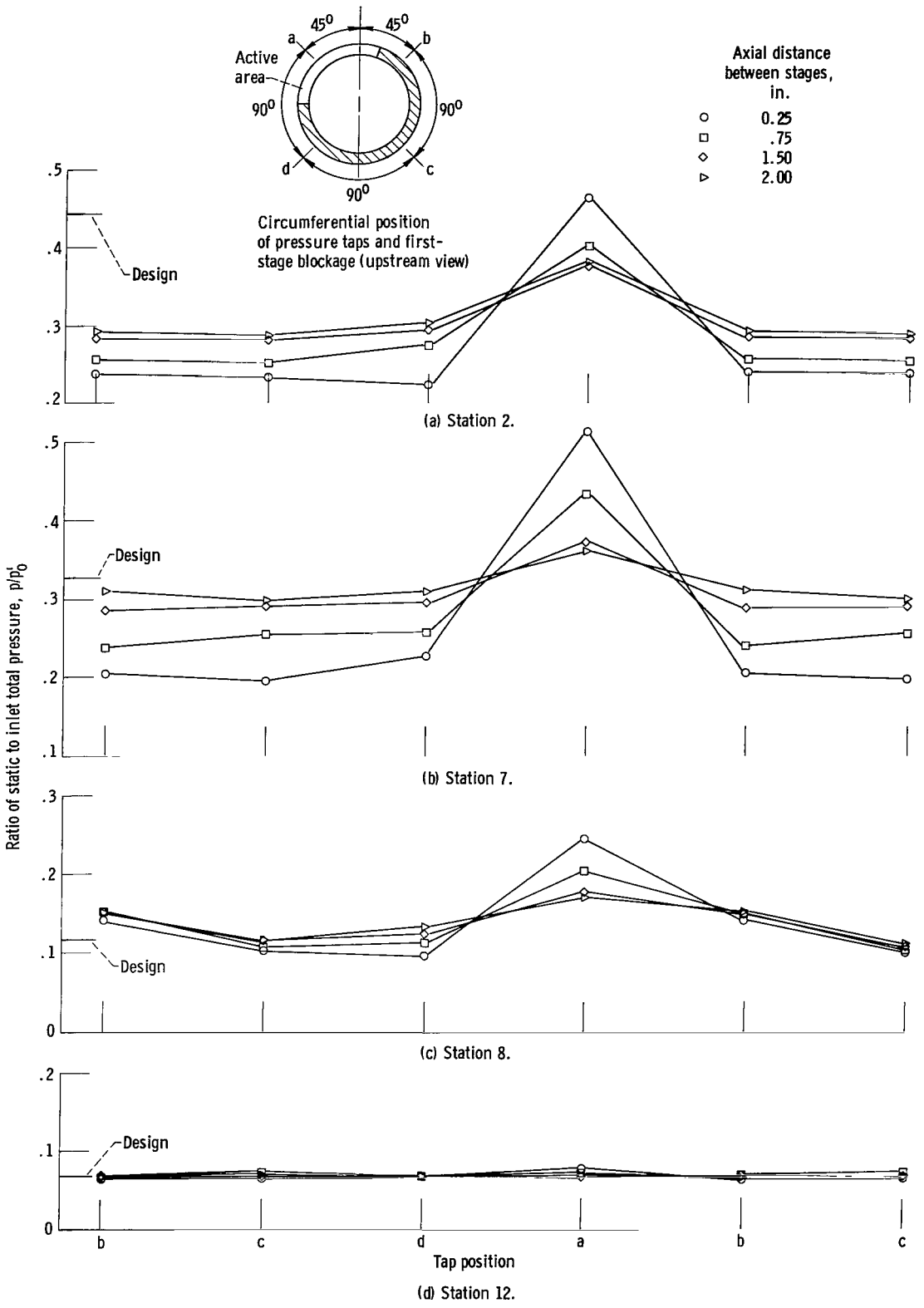

Figure 12. - Circumferential variation of static pressure at design speed and overall pressure ratio.

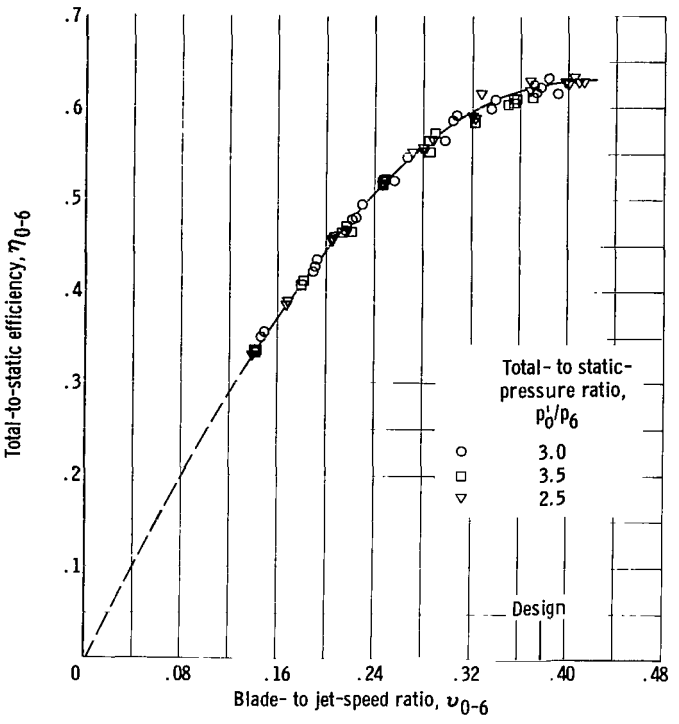

Figure 13. - Performance characteristics of first stage.

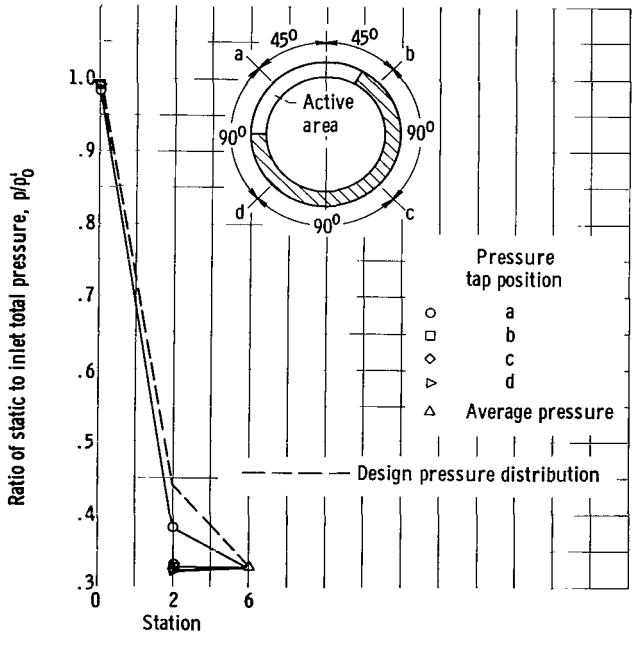

Figure 14. - Variation of static pressure for single-stage operation at design speed and overall pressure ratio.

are presented in figure 13. This figure shows the variation of total-to-static efficiency η_{0-6} with blade- to jet-speed ratios from about 0.12 to 0.42. At the design value of this ratio, 0.377, the total-to-static efficiency is 0.625 as compared with the design value of 0.645. Operation of the first stage at the design value of rotative speed and pressure ratio resulted in an equivalent specific work output $\Delta h/\theta_{cr}$ of 21.2 Btu per pound as compared with the design value of 21.8.

An average value of choking equivalent weight flow of 0.061 pound per second was obtained, which agrees with the results obtained in the two-stage investigation.

The pressure distribution is shown in figure 14, wherein the ratio of static to inlet total pressure is shown for each of the axial stations and for each of the four circumferential tap locations a, b, c, and d. As was found for the two-stage operation, the pressure distribution indicates an overexpanded stator and less than design reaction across the rotor. It also further substantiates the conclusion drawn from the two-stage investigation that the rotor throat area is too large. Figure 15 presents the ratio of static pressure at tap position a to inlet total pressure for stations 1 and 2 as a function of pressure ratio across the stage. The curve for station 2 shows a decrease in static pressure with an increase in overall pressure ratio, which generally indicates an unchoked rotor. At the larger pressure ratios, however, the slope of the curve indicates that the active section of the rotor

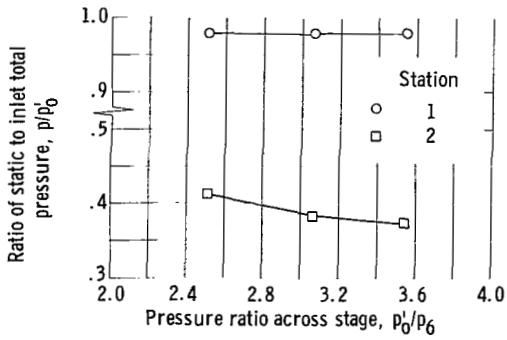

Figure 15. - Variation of static pressure with overall pressure ratio for single-stage operation at design speed. Active area, tap position, a.

operated near the choked condition.

The performance of the second stage was calculated by using the results presented for the single- and two-stage units. The work output of the single-stage unit for a given operating point of the two-stage unit was determined from the blade speed, the inlet total pressure, and the static pressure measured in the active area directly behind the rotor. This work output was calculated from the efficiency as read off the single-stage performance curve in figure 13. Both the work output and the static-to-static pressure ratio for the second stage were thus determined, and from them the effiency was calculated. It should be noted that the efficiency thus calculated was based on the static-to-static pressure ratio. Since the design conditions specify a static-to-total pressure ratio of 0.92 at the second stage inlet, the calculated value of efficiency is slightly larger than a value based on the total-to-static pressure ratio. The method used for the calculation of the efficiency, however, does not change the effect of axial distance between stages on second stage efficiency. Figure 16 presents the results of these calculations for each of the six axial distances between stages. The efficiency increases from a value of 0.528 at a distance of 0.25 inch to a value of 0.60 at a distance of 2.00 inches. The increase in efficiency of 0.072 for the second stage as the distance between stages was increased from 0.25 to 2.00 inches is indicative of the effect of partial admission in the first stage on the performance of the second stage. It should be noted that the observed change in efficiency with distance should not be generalized since changes in the inlet arc of admission can have significant effects on these results.

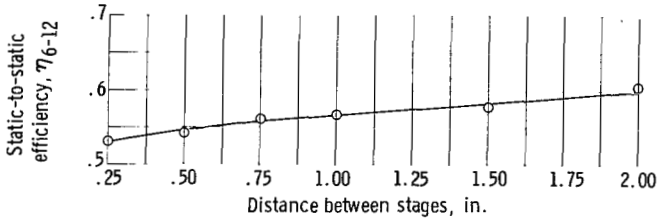

Figure 16. - Variation of calculated second-stage static efficiency with axial distance between stages at design blade- to jet-speed ratio.

SUMMARY OF RESULTS

The design and experimental investigation of a 3.75-inch-mean-diameter two-stage turbine are presented. The turbine had 31.3-percent admission in the first stage and full admission in the second stage. Overall and second-stage performance characteristics were obtained for axial distances between stages of 0.25, 0.50, 0.75, 1.00, 1.50, and 2.00 inches. First-stage performance data were also obtained and are included herein. The principal results of the investigation are the following:

1. For the range of axial distances considered in the two-stage investigation, there is an increase in efficiency with an increase in distance between stages at all values of blade- to jet-speed ratio. At the design value of blade- to jet-speed ratio of 0.27, the static efficiency increased from a value of about 0.584 at a distance of 0.25 inch to a value of 0.655 at a distance of 2.00 inches. At the latter point of operation the design value of overall equivalent specific work output of 43.6 Btu per pound was obtained.

2. The design pressure distribution through the turbine was not obtained because of the poor circumferential distribution of flow downstream of the first-stage stator and a slight mismatch between stator and rotor flow areas. As the distance between stages was increased, however, the circumferential distribution of flow improved, and the pressure distribution approached the design value.

3. First-stage operation at the design value of blade- to jet-speed ratio resulted in a static efficiency of 0.625 as compared with the design value of 0.645.

4. The performance of the second stage as calculated from the results of the two-stage and single-stage investigations showed an increase in efficiency from a value of 0.528 at an axial distance of 0.25 inch between stages to a value of 0.600 at a distance of 2.00 inches.

CONCLUDING REMARKS

It can be concluded from the results of this investigation that the performance of multistage partial-admission turbines requiring large increases in arc of admission between successive stages may be penalized if sufficient spacing between stages is not provided to allow for adequate redistribution of the flow. If sufficient spacing cannot be utilized because of mechanical limitations, the attendant penalty can be severe and should be considered in establishing the expected efficiency. In such cases this penalty can be reduced by a reduction in the required amount of flow spreading between stages through a compromise between arc of admission and blade height.

Lewis Research Center
National Aeronautics and Space Administration
Cleveland, Ohio, February 27, 1964

REFERENCES

1. Stewart, Warner L.: Analytical Investigation of Multistage-Turbine Efficiency Characteristics in Terms of Work and Speed Requirements. NACA RM E57K22b, 1958.

2. Wong, Robert Y., and Monroe, Daniel E.: Investigation of a 4.5-Inch-Mean-Diameter Two-Stage Axial-Flow Turbine Suitable for Auxiliary Power Drives. NASA MEMO 4-6-59E, 1959.

3. Stewart, Warner L., Wong, Robert Y., and Evans, David G.: Design and Experimental Investigation of Transonic Turbine with Slight Negative Reaction Across Rotor Hub. NACA RM E53L29a, 1954.

4. Kofskey, Milton G.: Experimental Investigation of Three Tip-Clearance Configurations Over a Range of Tip Clearance Using a Single-Stage Turbine of High Hub- to Tip-Radius Ratio. NASA TM X-472, 1961.

5. Nusbaum, William J., and Holeski, Donald E.: Cold-Air Investigation of Prototype Snap-8 Turbine. NASA TN D-1529, 1962.

6. Wong, Robert Y., and Nusbaum, William J.: Air-Performance Evaluation of a 4.0-Inch-Mean-Diameter Single-Stage Turbine at Various Inlet Pressures from 0.14 to 1.88 Atmospheres and Corresponding Reynolds Numbers from 2500 to 50,000. NASA TN D-1315, 1962.

NASA-Langley, 1964 E-2236

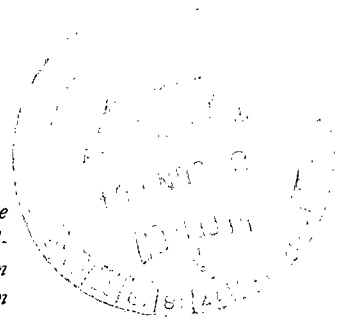

"The aeronautical and space activities of the United States shall be conducted so as to contribute . . . to the expansion of human knowledge of phenomena in the atmosphere and space. The Administration shall provide for the widest practicable and appropriate dissemination of information concerning its activities and the results thereof."

—NATIONAL AERONAUTICS AND SPACE ACT OF 1958

NASA SCIENTIFIC AND TECHNICAL PUBLICATIONS

TECHNICAL REPORTS: Scientific and technical information considered important, complete, and a lasting contribution to existing knowledge.

TECHNICAL NOTES: Information less broad in scope but nevertheless of importance as a contribution to existing knowledge.

TECHNICAL MEMORANDUMS: Information receiving limited distribution because of preliminary data, security classification, or other reasons.

CONTRACTOR REPORTS: Technical information generated in connection with a NASA contract or grant and released under NASA auspices.

TECHNICAL TRANSLATIONS: Information published in a foreign language considered to merit NASA distribution in English.

TECHNICAL REPRINTS: Information derived from NASA activities and initially published in the form of journal articles.

SPECIAL PUBLICATIONS: Information derived from or of value to NASA activities but not necessarily reporting the results of individual NASA-programmed scientific efforts. Publications include conference proceedings, monographs, data compilations, handbooks, sourcebooks, and special bibliographies.

Details on the availability of these publications may be obtained from:

SCIENTIFIC AND TECHNICAL INFORMATION DIVISION

NATIONAL AERONAUTICS AND SPACE ADMINISTRATION

Washington, D.C. 20546